Phys Chem Minerals (2002) 29: 181–187
DOI 10.1007/s00269-001-0219-1
© Springer-Verlag 2002

ORIGINAL PAPER

L. Liu · C.-C. Lin · T. P. Mernagh · T. Inoue

Raman spectra of hydrous γ-Mg_2SiO_4 at various pressures and temperatures

Received: 27 April 2001 / Accepted: 12 September 2001

Abstract One well-defined OH Raman band at 3651 ± 1 cm^{-1} and one weak feature near 3700 ± 5 cm^{-1} are recognized for the hydrous γ-phase of Mg_2SiO_4. Like the hydrous β-phase, the H_2O content in the γ-phase shifts most of the corresponding silicate modes towards lower frequencies. Variations in Raman spectra of the hydrous γ-phase were investigated up to about 200 kbar at room temperature and in the range 81–873 K at atmospheric pressure. Unlike the anhydrous γ-phase, which remains intact up to at least 873 K, the hydrous γ-phase sometimes converts to a defective forsterite structure above 800 K. Although the hydrous γ-phase remains intact up to at least 800 K, Raman signals of the OH bands disappear completely above 423 K. The Raman frequency of the well-defined OH band decreases linearly with increasing temperature between 81 and 423 K. In the region of the silicate vibrations, the Raman frequencies of the two most intense bands increase nonlinearly with increasing pressure, and decrease with increasing temperature. The frequencies for all other weak bands, however, decreased linearly with increasing temperature. The latter most likely reflects the larger scatter of the data for the weak bands.

Keywords Hydrous γ-Mg_2SiO_4 · Raman spectrum · Pressure dependence · Temperature dependence

L. Liu (✉) · C.-C. Lin
Institute of Earth Sciences, Academia Sinica,
Nankang, Taipei, Taiwan, ROC
e-mail: lliu@earth.sinica.edu.tw

T. P. Mernagh
Australian Geological Survey Organisation, Canberra,
ACT, 2601 Australia

T. Inoue
Department of Earth Sciences, Ehime University,
Matsuyama 790, Japan

Introduction

It is widely accepted that olivine, $(Mg, Fe)_2SiO_4$, is probably the most abundant mineral in the Earth's upper mantle. Magnesium-rich olivine transforms to the β-and γ-phases at pressures and temperatures relevant to the transition zone of the mantle (e.g., Liu and Bassett 1986). Thus, these high-pressure phases are believed to be the most abundant minerals in the transition zone. It has been estimated that the Earth's mantle might contain more than five times its present water content in the near-surface geochemical reservoirs (hydrosphere + crust) (Liu 1987). Although there are many dense hydrous magnesium silicates (e.g., phases A, B, C, etc.), which accommodate H_2O and are known to be stable at the pressure and temperature conditions relevant to the Earth's mantle, it would be rather significant if the β-and γ-phases could also accommodate H_2O. Considering the electrostatic potential and the polyhedral coordination, Smyth (1987) suggested that the O(1) sites in the β-phase structure may be a host for hydroxyl groups. If all of the O(1) sites are assumed to be replaced by OH, the H_2O content in the hypothetical hydrous β-phase would be 3.3 wt% according to Inoue et al. (1995), who have successfully synthesized several hydrous β-phases which contain up to 3 wt% H_2O. In hydrothermal annealing experiments with single crystals of San Carlos olivine, one of the γ-phase crystals quenched from 195 kbar and 1100 °C dissolved some 2.6 wt% H_2O (Kohlstedt et al. 1996). The pure magnesium hydrous γ-phase was later synthesized at 190 kbar and 1300 °C by Inoue et al. (1998). Like anhydrous γ-Mg_2SiO_4, the hydrous γ-phase still possesses a cubic structure, but its Mg/Si ratio is approximately 1.95 ± 0.02 (Inoue et al. 1998).

Raman spectra of the hydrous β-phase at various pressures and temperatures have been previously reported by Liu et al. (1998a). The results of a similar study of the hydrous γ-phase are reported in the present study. The data thus obtained were also compared with

those of the anhydrous γ-phase to see the effect of H_2O substitution on the Raman shift at various pressures and temperatures.

Experimental procedure

Two large single crystals of the hydrous γ-phase were synthesized at 190 kbar and 1300 °C for 60 min in a multianvil press in SUNY at Stony Brook. The starting materials were a mixture of $MgO:Mg(OH)_2:SiO_2 = 1:1:1$ in molar ratio. The polished surface of one single crystal was about 150×400 μm^2 and the other about 400×600 μm^2, and the depth of these crystals was estimated to be 100∼200 μm. A microfocused (50 μm) X-ray diffractometer study at the Ehime University showed that these crystals have the spinel structure. The results of electron microprobe analyses (EMPA) of the single crystals performed in Ehime University are close to an olivine stoichiometry with the Mg/Si = 1.88 ± 0.03, and the deficit of EMPA totals gave $H_2O = 2.7 \pm 0.9$ wt% from the average of 20 measurements, which were recalculated by assuming that the EPMA total of San Carlos olivine is 100% as reference. A secondary ion mass spectrometry study at the Tokyo Institute of Technology yielded $H_2O = 2.8 \pm 0.2$ wt%, which is in good agreement with the EMPA data. The chemical formula of the present sample is estimated to be approximately $Mg_{1.84}Si_{0.98}H_{0.42}O_4$.

Fourier-transform infrared spectroscopy with absorption mode (FTIR; Bruker EQUINOX 55, resolution = 2 cm^{-1}, 640 scans, and 1 s scan^{-1}) was also employed to confirm the quality of the sample. The sample for the FTIR study was prepared by pressing a single grain into a disk which is about 10∼20 μm in thickness and 250 μm in diameter. This disk was then sandwiched between two KBr disks, the total thickness of the sandwiched disk being about 100 μm. The unpolarized FTIR spectrum, shown in Fig. 1, is composed of peaks at 3420, 3145, 2911, 2513, and 2423 cm^{-1}. The strong peak at 3145 cm^{-1} is very close to that at 3120 cm^{-1} of the hydrous γ-phase observed by Bolfan-Casanova et al. (2000). The strong peak at 3345 cm^{-1} of the hydrous γ-phase observed by Kohlstedt et al. (1996) was not confirmed by the study of Bolfan-Casanova et al. (2000) and by this work.

In the high-pressure experiments, one or two small chips of the sample, approximately $20 \times 40 \times 50$ μm^3 in size, were placed inside the hole (100∼150 μm in diameter and 60∼80 μm in depth) in a hardened stainless steel gasket in a standard diamond anvil cell. The anvil faces are approximately 600 μm in diameter. Single crystal samples were set on top of ruby powder, and deionized water was used as a pressure medium. The whole assembly was then sealed by compressing the two diamond anvils. Pressures were measured using the ruby-fluorescence technique. The Raman spectra of the samples and the ruby-fluorescence spectrum were measured at the same spot. This procedure tends to reduce the errors caused by the pressure gradients across the samples. Although H_2O freezes at 9.3 kbar at room temperature, the hydrostatic behavior of ices VI and VII is about the same as an ethanol-methanol mixture at pressures below 100 kbar and is superior to both solid CO_2 and an ethanol-methanol mixture in the pressure region 100 to 500 kbar or greater. The hydrostaticity of the H_2O medium at high pressures can be estimated from the shape of fluorescence bands of ruby, and was judged to be acceptable. It was also noted that the Raman bands of water and ices VI and VII are weak and broad at room temperature and that the Raman bands of H_2O do not interfere with the recognition of sample signals.

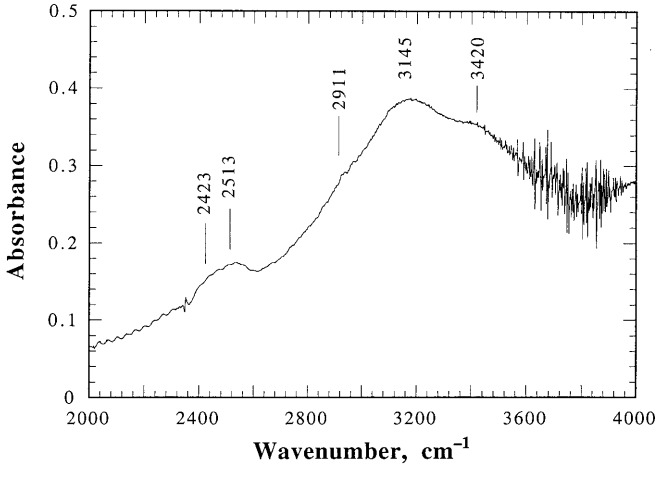

Fig. 1 Unpolarized FTIR spectrum of the hydrous γ-phase used in this study

In the temperature variation experiment, sample chips of approximately 20∼80 μm in size were placed at the center of a 16-mm-diameter crucible which has a sapphire window as the base. The crucible was then placed directly on a small silver block in a Linkam THM 600 heating/freezing stage which consists of a double-walled, anodized aluminum thermal cell. The cell can be purged with dry nitrogen to exclude moisture and air. Low temperatures are obtained by pumping liquid nitrogen through an annulus in the silver block, and a resistance heater opposes the cooling effect of the nitrogen to yield the desired temperature. In the heating mode only the resistance heater is used along with water cooling of the cell. The temperature is monitored by a platinum resistance thermometer attached to the heater. The temperature control unit is completely automatic and can be programmed to maintain any desired temperature or to change temperature at a constant rate.

In both modes, the sample temperature is controlled by thermal conduction between the sample and the silver block. The stage has been calibrated at both high and low temperatures by observing the phase changes in synthetic fluid inclusions placed in the center of the crucible. A more detailed description of the experimental procedures was given earlier (Liu and Mernagh 1994). Horizontal thermal gradients may lead to errors of up to 1% in temperature measurement. After varying the temperature, the samples were kept at the new temperature for at least 5 min before recording the Raman spectrum, in order to allow the samples to reach thermal equilibrium.

Laser Raman spectra for the hydrous γ-phase at ambient pressure and various temperatures were recorded from 100 to 4000 cm^{-1} on a Dilor SuperLabram spectrometer equipped with a holographic notch filter, 600 and 1800 g mm^{-1} gratings, and a liquid N_2 cooled, 2000×450 pixel CCD detector. The crystals were illuminated with 514.5 nm laser excitation from a Spectra Physics model 2017 argon ion laser, using 5 mW power at the samples, and a single 60-s accumulation. In the temperature variation study, Raman spectra were recorded in two separate regions (100–1600 and 2700–4000 cm^{-1}), corresponding to the spectral coverage on the detector produced by the 1800 g mm^{-1} grating of the spectrometer. The grating was kept stationary while the temperature was varied. This should provide the most accurate means for directly comparing the variation of frequency with temperature. A 50X ULWD Olympus microscope objective was used to focus the laser beam and collect the scattered light.

The pressure variation study was carried out on a Renishaw-2000 Raman microprobe, and the excitation source was a Coherent INNOVA 2W argon ion laser. The spectra were recorded with a 25X UM Leitz microscope objective and at 300 s integration time with 60 mW power on the sample. The focused laser spot on the sample was approximately 2–3 μm in diameter in the temperature experiment and about 2–4 μm in diameter in the pressure experiment. Wavenumbers are accurate to ±1 cm^{-1} as determined by plasma and neon emission lines. The frequency of each Raman band was obtained by Lorentzian curve fitting using a computer software.

Ambient Raman spectrum

The Raman spectrum of the hydrous γ-phase has not been previously reported. The ambient Raman spectra are similar to those shown at 273 K in Figs. 2a and 2b.

Raman frequencies corresponding to the OH groups are characterized by one well-defined band at 3651 ± 1 cm^{-1} and one weak feature near 3700 ± 5 cm^{-1}. The former was observed in most cases, and the latter occurred sporadically. The peak near 3651 cm^{-1} is nearly identical to the A_{1g} OH-mode of brucite (3652 cm^{-1}). The possibility that this band might be due to brucite can be ruled out by the following evidence. First, both X-ray diffraction and EMPA studies (see Experimental Procedure) show that there is no detectable amount of brucite in the sample used in the present study. Therefore, the strong OH peak near 3651 cm^{-1}, which was observed ubiquitously in the sample, cannot possibly be due to brucite. Second, this band can be observed in clear and transparent parts of a large crystal. Impurities such as small crystals should be optically observable in this circumstance. Thirdly, where this peak was observed, the strong lattice modes of brucite at 443 and 280 cm^{-1} were not observed. (Occasionally, a very weak band near 446 cm^{-1} can be observed in the present sample, as indicated in Table 1. However, the intensity of this band is too weak to assign it to the strong 443 cm^{-1} band of brucite). Fourth, the Raman frequency for the A_{1g} OH-mode of brucite was observed to decrease with increasing pressure (Duffy et al. 1995). Although the temperature variation of Raman spectra of brucite is not available, it is most likely that Raman frequency for the A_{1g} OH-mode of brucite should increase with increasing temperature. In the present study, we found that the Raman frequency for the 3651 cm^{-1} band decreased with increasing temperature (see Fig. 2a and later discussion).

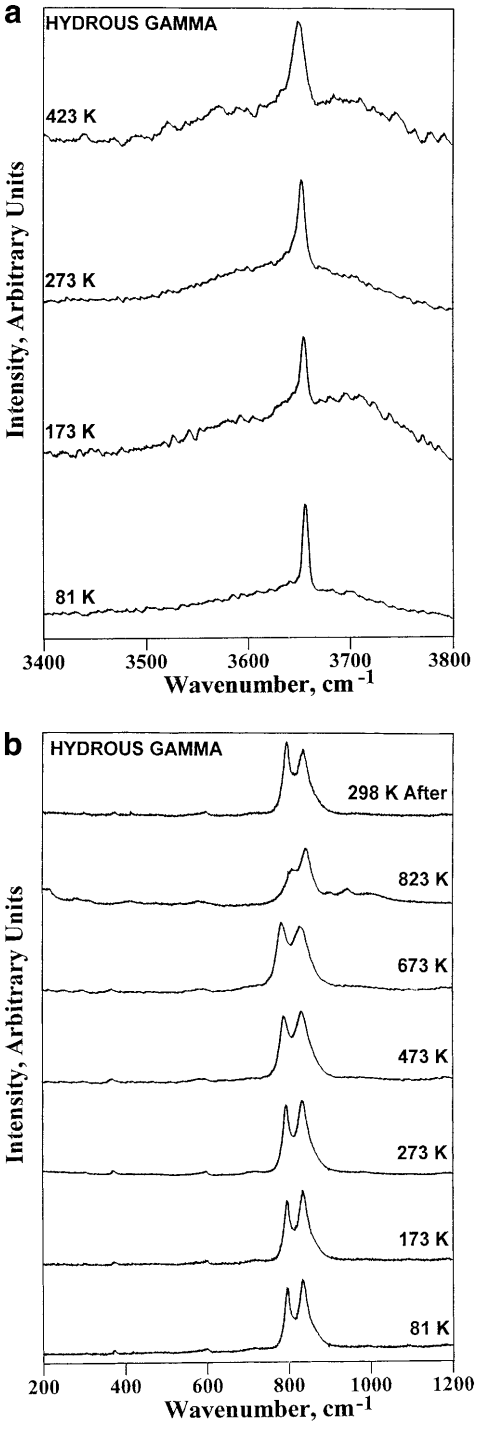

Fig. 2a, b Selected Raman spectra of the hydrous γ-phase at various temperatures. The spectra were obtained using 514.5-nm excitation at 50 mW power. **a** In the range 3400 ~ 3800 cm^{-1} and **b** 200 ~ 1200 cm^{-1}

The frequencies of the Raman bands below 1400 cm^{-1} of the present sample are compared with those of the anhydrous γ-phase in Table 1. There are only five Raman bands (two strong and three very weak) in the anhydrous γ-phase (McMillan and Akaogi 1987). The Raman spectrum of the anhydrous γ-phase is nearly the same as those shown in Fig. 2b, except that the hydrous γ-phase possesses a few extra weak bands (see Table 1). On the basis of symmetry analysis, Chopelas et al. (1994) concluded that there should be only five Raman bands for a cubic spinel structure of γ-Mg_2SiO_4. The fact that more than five bands are observed in this region suggests that the hydrous γ-phase may in reality not be of a cubic structure as implied by the X-ray data of Inoue et al. (1998). However, the two bands near 1092 and 988 cm^{-1} in Table 1 may also be due to in-plane and out-of-plane bending vibrations of the OH-stretching band at 3651 cm^{-1}. Like the pair of anhydrous and hydrous β-phases (Liu et al. 1998a), the frequencies of most of the Raman bands of the hydrous γ-phase shift slightly towards lower frequencies, in comparison with those of the anhydrous γ-phase. The reasons for the changes in the Raman spectra in β-phase have been discussed in detail by Mernagh and Liu (1996). The same may apply to the γ-phase here.

Pressure dependence of Raman spectra

Despite numerous attempts, the OH-stretching bands for the hydrous γ-phase were not observed in the high-pressure cell in the present study. In the silicate mode region, like the anhydrous γ-phase, only the two most

Table 1 Constants determined in $\Delta v_i = a_i + b_i P + c_i P^2$ at room temperature and in $\Delta v_i = a_i + b_i T + c_i T^2$[a] at atmospheric pressure for the hydrous γ-phase

Observed $\Delta v_{i,\mathrm{amb}}$		$\Delta v_i = a_i + b_i T + c_i T^2$					
Anhydrous	Hydrous	$^*\Delta v_{i,\mathrm{amb}}$[b]	$-(\partial v_i/\partial T)_P \times 10^2$	a_i	$-b_i \times 10^2$	$-c_i \times 10^5$	R^2[c]
	3697						
	3651	3652	2.41	3659.4	2.411	–	0.987
	1092	1092	0.4	1093.0	0.38	–	0.351
	–	988	2.4	995.1	2.43	–	0.916
	866 sh	–					
836	835	835	0.875	835.7	−0.179	1.768	0.990
795	795	795	1.748	796.6	−0.315	3.461	0.989
	713	710	2.97	718.7	2.97	–	0.606
600	595	594	2.78	602.1	2.78	–	0.825
	578	578	1.4	581.9	1.37	–	0.867
	446	–					
370	372	373	1.47	377.2	1.47	–	0.946
302	301	301	0.8	304.0	0.84	–	0.662
		$\Delta v_i = a_i + b_i P + c_i P^2$					
836	835	834		834.3	−46.0	56.6	0.996
795	795	794		794.1	−58.7	92.1	0.994

[a] Both Δv_i and a_i are in cm^{-1}, T in K, P in kbar, and the constants b_i and c_i have the corresponding units
[b] Both $^*\Delta v_{i,\mathrm{amb}}$ and $(\partial v_i/\partial T)_P$ were calculated at ambient condition, and for high-pressure data $b_i = (\partial v_i/\partial P)_T$ at ambient condition
[c] R^2 is the coefficient of correlation

intense bands (835 and 795 cm^{-1}) could be reliably measured. Four separate experimental runs were conducted, and the combined data are displayed in Fig. 3. As observed in earlier studies (e.g., Liu and Mernagh 1993), the error increases with increasing pressure. Nevertheless, it is clear that the frequencies of both intense bands increase nonlinearly with increasing pressure. These two bands cannot be recognized beyond 200 kbar, but they reappeared when pressure was released, indicating that the disappearance of Raman signals at pressures greater than 200 kbar is not caused by the formation of an amorphous phase. The trend of the weak shoulder at 866 cm^{-1} can hardly be established. The constants in the quadratic regressions of these data are given in Table 1, and the regressions are shown as solid lines in Fig. 3.

The values of $(\partial \mathrm{v}_i/\partial P)_T$, or b_i values in Table 1, for the 835 and 795 cm^{-1} bands were also compared with those for their corresponding Raman bands in anhydrous γ-phase in Table 2. These values for the hydrous phase are some 10% greater than those for the anhydrous one. The mode vibrational frequencies of crystals depend on the bond length and bond angle, which change with the variation of volume. Thus, the high-pressure Raman data given in Table 2 suggest that the hydrous γ-phase may be slightly more compressible than the anhydrous γ-phase. Although this conclusion is the opposite of that observed between anhydrous and hydrous β-phases, it is consistent with the recent Brillouin scattering study of the hydrous γ-phase reported by Inoue et al. (1998). Thus, comparing with the data for anhydrous and hydrous β-phases, the presence of OH is not necessary to make nominally anhydrous silicates become more or less compressible. It seems to depend on

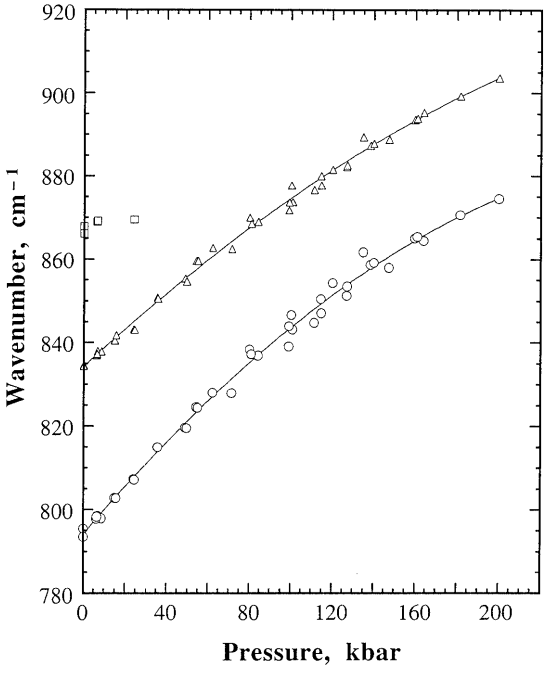

Fig. 3 Pressure dependence of the Raman bands of the hydrous γ-phase at room temperature. The *lines* are quadratic regressions of the data

what positions the OH ions occupy in the crystal. According to Smyth (1987) and Inoue et al. (1995), the O(1) sites in the β-phase structure may be replaced by OH. Thus, the hydrogen bond may have strengthened the crystal structure, making the hydrous phase less compressible in the β-phase structure. The structure of the hydrous γ-phase has not yet been studied, and it is rather difficult to draw a parallel comparison between

Table 2 Comparison of ambient pressure and temperature dependency of Raman frequencies between anhydrous and hydrous γ-phases of Mg_2SiO_4

Anhydrous			Hydrous[c]		
$\Delta\nu_{o,i}$ cm^{-1}	$(\partial\nu_i/\partial P)_T$[a] cm^{-1} $kbar^{-1}$	$(\partial\nu_i/\partial T)_P$[b] cm^{-1} deg^{-1}	$\Delta\nu_{o,i}$ cm^{-1}	$(\partial\nu_i/\partial P)_T$ cm^{-1} $kbar^{-1}$	$(\partial\nu_i/\partial T)_P$ cm^{-1} deg^{-1}
836	0.41 (0.431)	−0.013	835	0.460	−0.0088
795	0.54 (0.551)	−0.0299	795	0.587	−0.0175

[a] From Liu et al. (1994). The data in parentheses are from Chopelas et al. (1994)
[b] From Liu and Mernagh (1994)
[c] This work

the pairs of anhydrous-hydrous γ-phases and anhydrous-hydrous β-phases.

Temperature dependence of Raman spectra

Raman spectra of the hydrous γ-phase were recorded over the temperature range 81–873 K at atmospheric pressure in the present study. The lower temperature is limited by the liquid N_2 used to cool the sample stage, and the high temperature is limited by the instrument. In general, the resolution of the various Raman bands of the hydrous γ-phase observed in the temperature variation study is superior to that observed in the high-pressure experiment. Thus, more Raman bands for the hydrous γ-phase were measured in the temperature experiment.

As a general rule, the quality of spectrum has been improved at lower temperatures (see Fig. 2). The OH-stretching bands can hardly be recognized when the temperature increased above 423 K, though the hydrous γ-phase remained intact up to 873 K. Not all of the single crystals of the hydrous γ-phase can sustain the highest temperatures of the present study. It was observed that small grains of the single crystal converted to defective forsterite at temperatures greater than 800 $\sim$ 825 K. Only the larger grains ($> \sim 50$ μm in size) of the single crystal remained intact to 873 K. This parallels what has been observed in phase D (Liu et al. 1998b). The recovered samples are very similar to the starting hydrous γ-phase at ambient conditions (see Fig. 2b).

The variations of all Raman modes of hydrous γ-phase with temperature are shown in Fig. 4, in which the size of the symbols roughly indicates the relative intensities of these modes. As shown in Fig. 4, the OH-stretching Raman band could be measured up to 423 K. Within the experimental uncertainties and the range investigated, the frequency of this band decreases linearly with increasing temperature. The variation of nine SiO_4 and lattice modes was also measured (Fig. 4). Except for the two most intense bands, which possess nonlinear behavior, the frequencies for all weak Raman bands of the hydrous γ-phase decrease linearly with increasing temperature. The linear behavior, however, may be due to the scatter of the data, which in turn is attributed to the weak intensities of these bands.

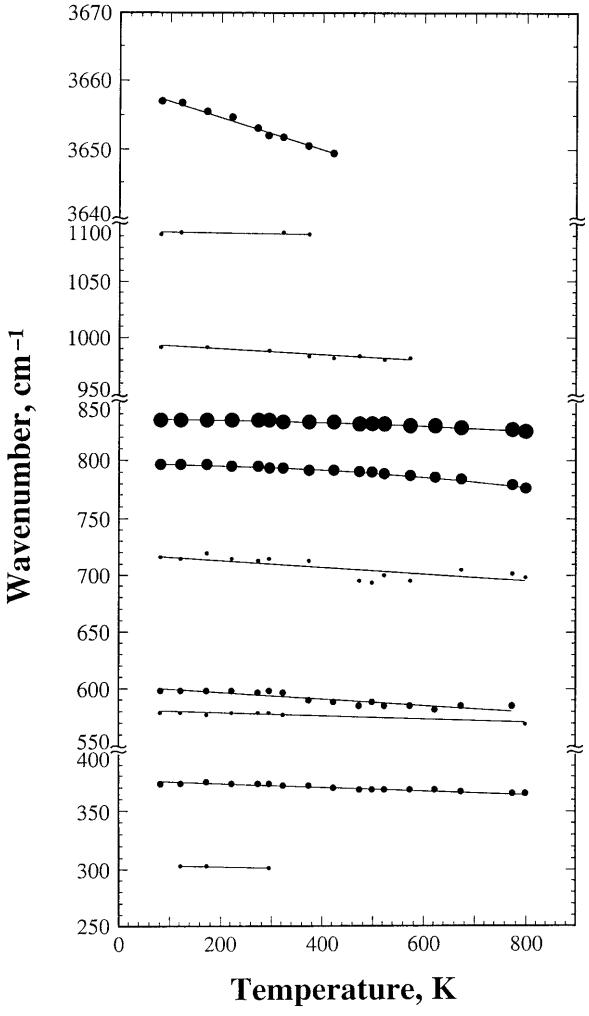

Fig. 4 Temperature dependence of the Raman bands of the hydrous γ-phase at atmospheric pressure. The *size of the symbols* roughly indicates the relative intensities of the bands. The *lines* represent the linear and quadratic regressions of the data

The values of $(\partial\nu_i/\partial T)_P$ derived by both linear and quadratic regressions of these modes are given in Table 1. The rates of change, $(\partial\nu_i/\partial T)_P$, determined for the two most intense Raman bands of the hydrous γ-phase were compared with those of the anhydrous γ-phase in Table 2, because only these two bands of the anhydrous γ-phase were reported. Note that the temperature dependences [or the values of $(\partial\nu_i/\partial T)_P$ in Table 2] of Raman modes of the hydrous γ-phase are some 30–40% smaller than those of the corresponding Raman modes of the anhydrous γ-phase. By adopting the same assumption that the mode vibrational frequencies of crystals depend mostly on the variation of volume, the temperature variation data of Table 2 suggest that the volume thermal expansivity for the hydrous γ-phase is smaller than that for the anhydrous γ-phase. This is the opposite behavior to the results of our studies of these two phases at high pressures described above.

The fact that the Raman frequency of the OH-stretching band of the hydrous γ-phase decreases with increasing temperature may imply that the opposite trend should be observed with increasing pressure. Unfortunately, we were unable to establish this in the present study. If the Raman frequencies of the OH bands of the hydrous γ-phase indeed increase with increasing pressure, then this variation is the opposite to that observed in the hydrous β-phase at high pressures. This fact may be relevant to our earlier discussion concerning the compressibilities of the anhydrous and hydrous β-and γ-phases.

Geophysical implications

Magnesium-rich olivine, or forsterite, is in general believed to be the most abundant mineral in the upper mantle. Kohlstedt et al. (1996) recently found that San Carlos olivine can contain up to 0.15 wt% H_2O at 120 kbar and 1100 °C in their hydrothermal annealing experiments. Although the H_2O contents of olivine in these high-pressure experiments are some 2 to 3 orders of magnitude higher than those found in natural olivine (contain $\sim$1 to 50 ppm H_2O by weight) reviewed by Bell and Rossman (1992), these OH concentrations in nominally anhydrous upper mantle minerals are still very limited and cannot be too significant to our understanding of the state of hydration of the mantle. However, phase E possesses features of brucite-type units (Kudoh et al. 1993), and it may be regarded as a hydrous forsterite from the viewpoint of its chemistry and Raman spectrum (Liu et al. 1997). Phase E contains some 15–18 wt% H_2O. If sufficient H_2O is available in the mantle, it is likely that most of the mantle olivine may convert to phase E. Phase E has been observed in various mineral assemblages which are stable at the various temperature and pressure conditions relevant to the Earth's mantle (Kanzaki 1991; Ohtani et al. 1995).

Both hydrous β- and γ-phases contain some 2.5 wt% H_2O. Anhydrous β- and γ-phases are the most abundant mineral phases in the nominally dry transition zone. Thus, the physical properties of phase E and hydrous β-and γ-phases are extremely important, if these phases are stable at the pressure and temperature conditions relevant to the mantle and if there is sufficient H_2O in the mantle. The elastic properties of phase E were briefly reported in an abstract (Bass et al. 1991). The compressional behavior of hydrous β-phase, on the other hand, was reported by Yusa and Inoue (1997) and the elastic moduli of hydrous γ-phase were reported by Inoue et al. (1998). These results all showed that the hydrous phases are more compressible than anhydrous phases (the bulk modulus is some 7.5% different between the pair of anhydrous and hydrous β-phases and some 19% different between the pair of anhydrous and hydrous γ-phases). On the other hand, the fact that the values of bulk modulus are nearly the same for both the hydrous β- and γ-phases (both have values of 1.55 Mbar) suggests that the results of these measurements are not entirely reliable, because the hydrous γ-phase is 4.2% denser than the hydrous β-phase and both phases have nearly the same chemical composition.

The results of the present study suggest that the hydrous γ-phase may be slightly more compressible than the anhydrous γ-phase, which is in line with the results of elastic modulus studies mentioned above whereas the earlier Raman studies of the anhydrous and hydrous β-phases indicated the opposite relationship. While the compressional behaviors between these anhydrous and hydrous phases remain unresolved at the moment, the density contrast between these anhydrous and hydrous phases is obvious. The ambient density of phase E is some 13.6% smaller than that of forsterite. The hydrous β-phase is some 5% less dense than the anhydrous β-phase, and the hydrous γ-phase is some 3% less dense than the anhydrous γ-phase. Thus, if the compressional behavior between these anhydrous and hydrous phases is similar, then the elastic waves may pass through these hydrous phases in the mantle faster than through the nominally dry mantle.

Acknowledgements T.P.M. publishes with permission of the Executive Director of Australian Geological Survey Organisation.

References

Bass JD, Kanzaki M, Howell DA (1991) Sound velocity and elastic properties of phase E: a high-pressure hydrous silicate. EOS 72: 499

Bell DR, Rossman GR (1992) Water in Earth's mantle: the role of nominally anhydrous minerals. Science 255: 1391–1397

Bolfan-Casanova N, Keppler H, Rubie DC (2000) Water partitioning between nominally anhydrous minerals in the MgO-SiO_2-H_2O system up to 24 GPa: implications for the distribution of water in the Earth's mantle. Earth Planet Sci Lett 182: 209–221

Chopelas A, Boehler R, Ko T (1994) Thermodynamics and behavior of γ-Mg_2SiO_4 at high pressure: implications for Mg_2SiO_4 phase equilibrium. Phys Chem Miner 21: 351–359

Duffy TS, Meade C, Fei Y, Mao HK, Hemley RJ (1995) High-pressure phase transition in brucite, $Mg(OH)_2$. Am Mineral 80: 222–230

Inoue T, Yurimoto H, Kudoh Y (1995) Hydrous modified spinel, $Mg_{1.75}SiH_{0.5}O_4$: a new water reservoir in the mantle transition region. Geophys Res Lett 22: 117–120

Inoue T, Weidner DJ, Northrup PA, Parise JB (1998) Elastic properties of hydrous ringwoodite (γ-phase) in Mg_2SiO_4. Earth Planet Sci Lett 160: 107–113

Kanzaki M (1991) Stability of hydrous magnesium silicates in the mantle transition zone. Phys Earth Planet Inter 66: 307–312

Kohlstedt DL, Keppler H, Rubie DC (1996) Solubility of water in the α, β and γ-phases of $(Mg, Fe)_2SiO_4$. Contr Mineral Petro 123: 345–357

Kudoh Y, Finger LW, Hazen RM, Prewitt CT, Kanzaki M, Veblen DR (1993) Phase E: a high-pressure hydrous silicate with unique crystal chemistry. Phys Chem Miner 19: 357–360

Liu L (1987) Effect of H_2O on the phase behavior of the forsterite-enstatite system at high pressures and temperatures and implications for the Earth. Phys Earth Planet Inter 49: 142–167

Liu L, Bassett WA (1986) Elements, oxides and silicates: high-pressure phases with implications for the Earth's interior. Oxford University Press, New york

Liu L, Mernagh TP (1993) Raman spectra of forsterite and fayalite at high pressures and room temperature. High Press Res 11: 241–256

Liu L, Mernagh TP (1994) Raman spectra of high-pressure polymorphs of Mg_2SiO_4 at various temperatures. High Temp-High Press 26: 631–637

Liu L, Mernagh TP, Irifune T (1994) High pressure Raman spectra of β-Mg_2SiO_4, γ-Mg_2SiO_4, $MgSiO_3$-ilmenite and $MgSiO_3$-perovskite. J Phys Chem Solids 55: 185–193

Liu L, Mernagh TP, Lin C-C, Irifune T (1997) Raman spectra of phase E at various pressures and temperatures with geophysical implications. Earth Planet Sci Lett 149: 57–65

Liu L, Mernagh TP, Lin C-C, Xu J, Inoue T (1998a) Raman spectra of hydrous β-Mg_2SiO_4 at various pressures and temperatures. In: Manghnani MH, Yagi T (eds) Properties of Earth and planetary materials at high pressure and temperature. American Geophysical Union, Washington, DC, pp 523–530

Liu L, Lin C-C, Irifune T, Mernagh TP (1998b) Raman study of phase D at various pressures and temperatures. Geophys Res Lett 25: 3453–3456

McMillan PF, Akaogi M (1987) The Raman spectrum of β-Mg_2SiO_4 (modified spinel) and γ-Mg_2SiO_4 (spinel). Am Mineral 72: 361–364

Mernagh PT, Liu L (1996) Raman and infrared spectra of hydrous β-Mg_2SiO_4. Can Mineral 34: 1233–1240

Ohtani E, Shibata T, Kubo T, Kato T (1995) Stability of hydrous phases in the transition zone and the upper most part of the lower mantle. Geophys Res Lett 22: 2553–2556

Smyth JR (1987) β-Mg_2SiO_4: a potential host for water in the mantle? Am Mineral 72: 1051–1055

Yusa H, Inoue T (1997) Compressibility of hydrous wadsleyite (β-phase) in Mg_2SiO_4 by high-pressure X-ray diffraction. Geophys Res Lett 24: 1831–1834